PERGAMON

International Journal of Solids and Structures 38 (2001) 1149–1167

INTERNATIONAL JOURNAL OF SOLIDS and STRUCTURES

www.elsevier.com/locate/ijsolstr

A study of strain-induced crystallization of polymers

I.J. Rao [a,*], K.R. Rajagopal [b]

[a] *Department of Mechanical Engineering, New Jersey Institute of Technology, Newark, NJ 07102, USA*
[b] *Department of Mechanical Engineering, Texas A&M University, College Station, TX 77843, USA*

Received 21 June 1999

Abstract

The response of polymers depends on their morphology. One of the challenges in modeling from a continuum perspective is how to incorporate the microstructural features into the homogenized continuum model. Here, we use a recent framework that associates different natural states and material symmetries with distinct microstructures of the body (Rajagopal, K.R., Wineman, A.S., 1992. International Journal of Plasticity 8, 385; Rajagopal, K.R., 1995. Reports of the Institute for Computational and Applied Mechanics, University of Pittsburgh; Rajagopal, K.R., Srinivasa, A.S., 1995. International Journal of Plasticity 11, 653; Rajagopal, K.R., Srinivasa, A.S., 1999. ZAMP 50, 459). We study the problem of strain-induced crystallization of polymeric materials, in particular, we study the problem of uniaxial stretching of polymeric materials and the subsequent crystallization and the predictions of the theory are compared with experimental results. © 2001 Published by Elsevier Science Ltd.

Keywords: Crystallization; Films; Stretching; PET; Polyethylene terephthalate; Polymer; Viscoelastic

1. Introduction

The mechanical behavior of polymers is closely related to their morphology, which in turn is determined by the conditions during processing. A number of polymers have the ability to crystallize forming materials that are semi-crystalline. The orientation of the crystals has a strong impact on the mechanical properties of the polymer. A majority of plastic products are manufactured by deforming the material at elevated temperatures to get it into the desired shape. Common examples of these types of operations include film blowing, fiber spinning and injection molding. In many of these applications, the formation of a highly oriented crystalline phase has a beneficial impact on the mechanical behavior of the material. In fibers, the formation of extended crystals in the direction of extension greatly increases the strength of the fiber. During the film-blowing operation, the melt is subjected to bi-axial extension, and the films have crystals oriented on the plane giving the film the desired mechanical properties. The application of polyester bottles

* Corresponding author. Tel.: +1-973-596-5601; fax: +1-973-642-4282.
E-mail address: raoi@njit.edu (I.J. Rao).

0020-7683/01/$ - see front matter © 2001 Published by Elsevier Science Ltd.
PII: S0020-7683(00)00079-2

to hold carbonated drinks has been possible due to the development of a special blow molding process which ensures that the polymer is bi-axially oriented. Orientation can also have a negative impact on the mechanical behavior of articles, e.g., in injection molding, the formation of a highly oriented outer layer can result in articles that are easily cleaved.

Polymers at elevated temperatures, above the melting temperature, are modeled as viscoelastic liquids. On cooling, depending on the molecular structure and the cooling rate, the solid that is formed can be either amorphous or semi-crystalline. Polymers with regular structures form semi-crystalline solids while those with irregular structures are unable to crystallize because the chains are too irregular to permit regular packing. The crystallization rate for polymers that do crystallize is usually observed to be zero at the melting temperature and at the glass transition temperature with a maximum at a temperature in between these two temperatures. The glass transition temperature is the temperature below which the polymer molecules lose their mobility and are "frozen" or vitrified. Polymers such as polyethylene in solid form are always semi-crystalline as their crystallization rates at temperatures below the melting point is very high, and it is not possible to cool the polymer rapidly enough to a temperature below the glass transition temperature without substantial crystallization taking place. For polymers such as polyethylene terephthalate (PET) which crystallize slowly, the melt has to be cooled slowly for substantial crystallization to take place. If these polymers are quenched to a temperature below their glass transition temperature, they remain in an amorphous state. When amorphous PET is subsequently deformed at temperatures just above the glass transition temperature, crystallization induced by the deformation takes place. Most PET articles are manufactured by deforming at these temperatures as the amount and orientation of the crystalline phase (and hence the mechanical properties of the final solid) can be controlled by imparting the right amount of deformation.

Classical works on phase transitions were devoted to studying problems, where conduction was the dominant mechanism (Stefan, 1891; Rubinstein, 1971; Crank, 1984). In the Stefan approach, temperature is the basic variable, and the fluid and solid are assumed to be quiescent. Another popular approach is the "phase-field" model which involves another parameter (other than temperature) called the order parameter. The order parameter has extreme values of $+1$ (for pure liquid) and -1 (for pure solid). The heat conduction equation is modified to incorporate the effect of the order parameter that leads to an additional equation whose origin can be traced to the Landau–Ginzburg theory of phase transitions (Landau, 1967). In most special problems, in polymer processing where the material is crystallizing while being deformed, mechanisms other than conduction such as convection in the fluid and deformation in the solid come into play. A deficiency of the above approaches is that these models are unable to predict the mechanical properties of the newly formed solid. The ability of a model to predict the properties of the newly formed solid is essential in most applications especially so in polymers where the properties of the final solid are affected by the processing conditions. Another drawback of these approaches is that they do not address the issue of symmetry, which is an important issue in phase transitions. When a material undergoes a transition from an amorphous to a crystalline phase, there is a discontinuous change in the symmetry group associated with the material. This manifests itself at the macroscopic level as an anisotropy in the mechanical response of the material. As anisotropy of the mechanical response enters the problem only when the kinematical fields in the amorphous and crystalline phase are taken into account, both the Stefan approach and the phase-field approach are inadequate for dealing with these issues. A continuum theory for phase transitions that can account for changes in symmetry has been developed by Baldoni and Rajagopal (1997). Their model assumes that the solid is isotropic, and its response is that of a neo-Hookean solid. Such a model is not appropriate for the modeling of the crystallization of polymeric melts that lead to semi-crystalline polymeric solids.

Experiments on crystallization in polymers have been done on a variety of polymer systems under different flow conditions. Here we present a brief overview of the different experiments and the main conclusions drawn from them. Experiments on crystallization in shearing flows between parallel plates have

been carried out by Haas and Maxwell (1969), Lagasse and Maxwell (1976), Katayama et al. (1976) and Nogami et al. (1977). Flow-induced crystallization has also been studied in rotational viscometers (Kobayashi and Nagasawa, 1970; Ulrich and Price, 1976; Sherwood et al., 1978; Wolcowicz, 1978). All these experiments indicate that the crystallization rate is enhanced due to the flow. At high rates of deformation, the time taken for crystallization was orders of magnitude less than for quiescent crystallization. Experiments in extensional flows have been reported by Mackley and Keller (1973), Mackley et al. (1973) and McHugh et al. (1993). These experiments also indicate that the rate of crystallization is accelerated due to the deformation. Experiments conducted in ducts of rectangular cross-section by Eder et al. (1989) indicate that the relaxation time of the melt has a strong effect on the thickness of the highly oriented layer, indicating the influence of relaxation effects on the crystallization process.

To characterize the process of crystallization, conditions at which nucleation takes place and the rate at which the crystalline phase grows have to be specified. Crystallization in polymers is traditionally modeled using the Avrami equation (Avrami, 1939). This equation is based on the theory of filling space through the nucleation and growth of one phase into another. A detailed description of the different variants of the Avrami equation can be found in the review by Eder et al. (1990) and the text on crystallization in polymers by Mandelkern (1964). Flow induced crystallization has been modeled by modifying the Avrami equation to account for enhanced crystallization rates due to the flow. In this approach, the effect of flow is built into the equation by the inclusion of an orientation factor, which depends on the flow (Ziabicki, 1974; Eder et al., 1990; Schultz, 1991).

From the experiments performed on phase transitions in polymers that crystallize, it is clear that the transition from an amorphous melt to a semi-crystalline solid is continuous, i.e., during this process, the material is a mixture of an amorphous polymer melt and a solid with a crystalline structure. On completion of crystallization, the solid formed is a mixture of a crystalline and amorphous solid. Orientation in the melt tremendously accelerates the process of phase transition. However, as the melt is a viscoelastic fluid, the orientation of the molecules can either build up or relax depending on the deformation history and the relaxation time of the melt. Orientation of the crystallites formed depends strongly on the orientation of the molecules in the melt just prior to crystallization.

In this paper, we develop a model for strain-induced crystallization in PET at temperatures above the glass transition temperature. PET is commonly used in the manufacture of bottles, films and fibers. The melting temperature of PET is 266°C and its glass transition temperature is 70°C. Since the rate of crystallization in quiescent, unoriented PET is slow, it can be quenched into an amorphous solid. Also, crystallization in quiescent unoriented PET is only significant at temperatures above 105°C. In the temperature range between the glass transition temperature and approximately 105°C, crystallization can be induced in amorphous PET by deformation. This has many practical advantages as the amorphous PET can be deformed so as to crystallize in a manner that gives the final product the desired mechanical properties. The blow molding of plastic bottles is an example of a process where amorphous PET is subjected to bi-axial extensions resulting in crystalline orientation. This orientation is essential for the bottles to have the required mechanical properties. Most products using PET are manufactured in this temperature range.

There have been numerous studies involving hot drawing of PET films (Buckley et al., 1996; Salem, 1998, 1992; Bourvellec and Beautemps, 1990a,b). The commonly done experiment is to stretch the film at a constant extension rate. In this type of extension there is a rapid increase in the stress after the onset of crystallization (Salem, 1992). Also, the onset of crystallization takes place at lower values of extension for higher extension rates. This is easily seen from the data points in Figs. 5 and 6. In practical applications where stretching is done between rollers rotating at different angular velocities, the stretching takes place under conditions of constant force, if the effects of inertia and drag forces are ignored. This has been simulated in the laboratory by Bourvellec and Beautemps (1990a,b) by subjecting a film to extension at a constant load. In this type of experiment, the material deforms till it reaches a plateau extension. For low loads, the material flows gradually, and crystallization does not take place till the material has deformed

considerably. At high loads, the material deforms rapidly, and crystallization is initiated earlier. Consequently, the plateau deformation is reached in a shorter time.

In this paper, we shall develop a model to simulate crystallization taking place in constant extension rate experiments and constant force experiments. We shall develop the theory within the framework of multiple natural configurations (Rajagopal, 1995). This approach has been used to explain the material response of a large class of materials under a unifying framework. Multi-network polymers (Rajagopal and Wineman, 1992), twinning (Rajagopal and Srinivasa, 1995), ligaments and tendons (Johnson et al., 1996), mental plasticity (Rajagopal and Srinivasa, 1998), materials undergoing solid to solid phase transitions (Rajagopal and Srinivasa, 1999) and viscoelastic liquids (Rajagopal and Srinivasa, 2000) have all been modeled within this framework, and classical elasticity and classical linearly viscous fluids arise naturally as sub-cases. We present the theory in a thermodynamic setting though the problem being solved is isothermal. We model the amorphous phase as a viscoelastic fluid and the crystalline phase as an elastic solid. An essential feature of irreversible processes, as is the one being studied here, is that the rate of dissipation be positive. For this problem, there is a rate of dissipation associated with the viscoelastic response of amorphous phase and also with the phase change (i.e., conversion of the material from amorphous to the crystalline phase). In addition to choosing forms for the Helmholtz potential for the amorphous material and the mixture of amorphous and crystalline material, we also need to choose forms for the rate of dissipation. The reduced energy-dissipation equation is then used to place restrictions on the form for the stress. We further assume that the viscoelastic behavior and the rate of crystallization take place in a manner so as to maximize the rate of dissipation. This assumption allows us to derive an equation for the rate of crystallization and equations for the evolution of the natural configuration associated with the viscoelastic fluid. This approach is the same as the one used to model twinning (Rajagopal and Srinivasa, 1995) and viscoelastic fluids (Rajagopal and Srinivasa, 1999). We model the amorphous PET as a viscoelastic fluid with two relaxation mechanisms. The crystalline phase is modeled as an anisotropic elastic solid. The anisotropy is induced from the deformation in the amorphous phase using the model developed by Rao and Rajagopal (2000). The model developed is used to solve problems of constant width extension of PET films. Two types of problems are solved, namely, constant extension rate stretching and constant force stretching. The results are compared with experimental data.

2. Preliminaries

Consider a body B in a configuration κ_{R}. Let $\mathbf{X}$ denote a typical position of a material point in κ_{R}. Let κ_t be the configuration at a time t, then the motion $\chi_{\kappa_{\mathrm{R}}}$ assigns to each particle in configuration κ_{R} a position in the configuration κ_t at time t, i.e.,

$$\mathbf{x} = \chi_{\kappa_{\mathrm{R}}}(\mathbf{X}, t). \tag{1}$$

The deformation gradient $\mathbf{F}_{\kappa_{\mathrm{R}}}$ is defined through

$$\mathbf{F}_{\kappa_0} := \frac{\partial \chi_{\kappa_{\mathrm{R}}}}{\partial \mathbf{X}}. \tag{2}$$

The left and right Cauchy–Green stretch tensors $\mathbf{B}_{\kappa_{\mathrm{R}}}$ and $\mathbf{C}_{\kappa_{\mathrm{R}}}$ are defined through

$$\mathbf{B}_{\kappa_{\mathrm{R}}} := \mathbf{F}_{\kappa_{\mathrm{R}}} \mathbf{F}_{\kappa_{\mathrm{R}}}^{\mathrm{T}}, \tag{3}$$

$$\mathbf{C}_{\kappa_{\mathrm{R}}} := \mathbf{F}_{\kappa_{\mathrm{R}}}^{\mathrm{T}} \mathbf{F}_{\kappa_{\mathrm{R}}}. \tag{4}$$

Any acceptable process has to satisfy the appropriate conservation laws. The conservation equations appropriate for studying the process of crystallization of PET are the conservation of mass, linear and angular

momentum and energy. As the problem we are studying is an isothermal problem, the energy equation need not be considered. We assume that the material is incompressible and that the density of the melt and the semi-crystalline solid are the same. This is an assumption made to simplify the problem, in actuality, a density change of a few percent is observed in the case of PET on transition from melt to solid, and this can be taken into account by appropriately modifying the theory. The conservation of mass for an incompressible material reduces to

$$\operatorname{div}(\mathbf{v}) = 0, \tag{5}$$

where $\mathbf{v}$ is the velocity. The conservation of linear momentum is

$$\rho\left[\frac{\partial \mathbf{v}}{\partial \mathbf{t}} + [\nabla \mathbf{v}]\mathbf{v}\right] = \operatorname{div}\mathbf{T} + \rho\mathbf{g}, \tag{6}$$

where $\mathbf{g}$ is the acceleration due to gravity and ρ is the density. For an incompressible material, the stress tensor $\mathbf{T}$ reduces to

$$\mathbf{T} = -p\mathbf{I} + \mathbf{T}^{\mathrm{E}}, \tag{7}$$

where p is the Lagrange multiplier due to the constraint of incompressibility, and $\mathbf{T}^{\mathrm{E}}$ is the constitutively determined extra stress. In this work, we use the reduced energy-dissipation equation to place restrictions on the constitutive equations. The reduced energy-dissipation equation for an isothermal process is

$$\mathbf{T}\cdot\mathbf{L} - \rho\dot{\psi} = \rho\theta\xi \equiv \zeta \geqslant 0, \tag{8}$$

where ψ is the Helmholtz potential, $\mathbf{L}$ is the velocity gradient, i.e., $\mathbf{L} = \operatorname{grad}\mathbf{v}$, ξ is the rate of entropy production and ζ is the rate of dissipation. Both ξ and ζ are constrained to be non-negative for an acceptable process.

The modeling of crystallization during film stretching can be separated into two main categories, namely, the modeling of the amorphous polymer prior to the onset of crystallization and the semi-crystalline polymer after crystallization begins.

3. Modeling the amorphous phase

PET in the temperature range of interest for this work (just above the glass transition temperature) is in the rubbery flow region. At these temperatures, for rapid deformations, the material behaves elastically like rubber while for slow processes, the material flows like a fluid. We model the amorphous region as a viscoelastic fluid using a rate type model. The derivation of the constitutive equations for the stress in a viscoelastic fluid closely follows the work of Rajagopal and Srinivasa (2000) based on the theory of evolving natural configurations. In this approach, the Helmholtz potential and the stress in the fluid are determined from the mapping between the tangent spaces of the natural configuration of the fluid at a material point to the current configuration occupied by it. In Fig. 1, κ_{R} is a reference configuration, $\kappa_{\mathrm{c}(t)}$ is the configuration currently occupied by the material and $\kappa_{\mathrm{p}(t)}$ is the natural configuration associated with the material. It is possible for the material to possess more than one natural configuration, and in polymeric materials with more than one relaxation mechanism, it is common to use models with more than one relaxation time. These models with multiple relaxation times are equivalent to viscoelastic fluid models with multiple sets of natural configurations.

To model PET at these elevated temperatures, we assume that the behavior is characterized by two independent relaxation mechanisms, i.e., it has two natural configurations corresponding to the current deformed configuration (Fig. 2). We could think of the viscoelastic material as a mixture of two materials

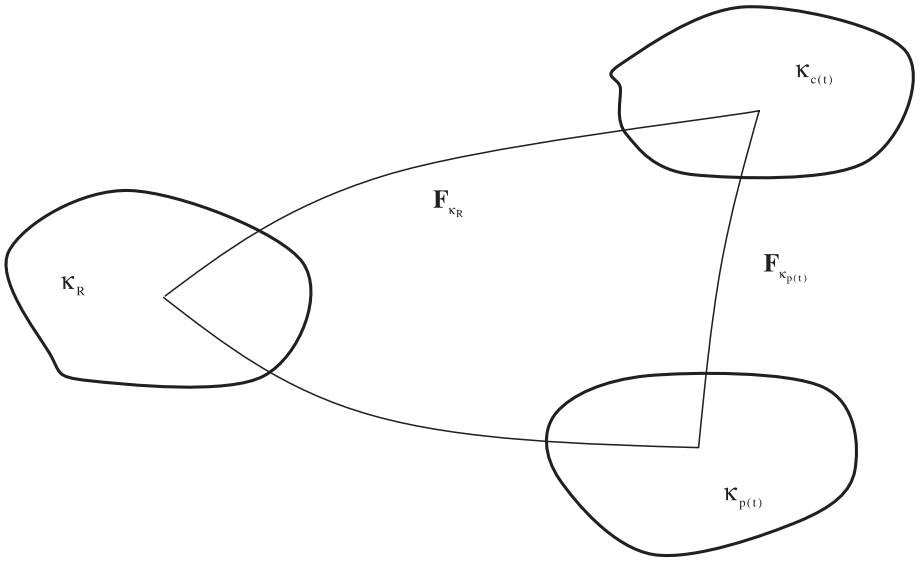

Fig. 1. Natural configurations associated with a viscoelastic fluid having a single relaxation mechanism.

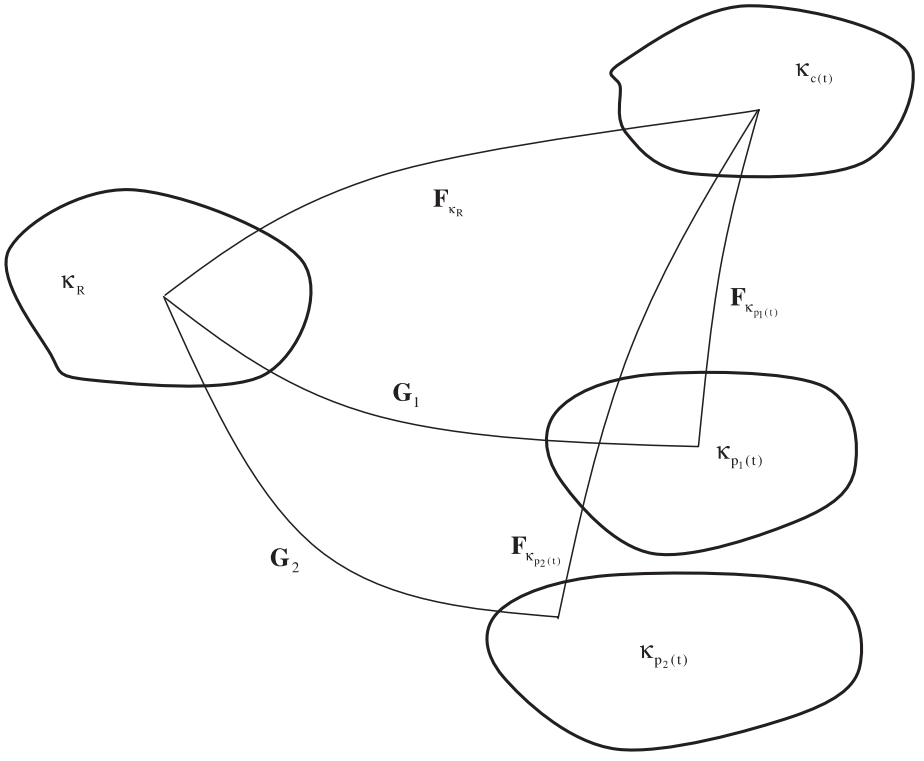

Fig. 2. Natural configurations associated with the amorphous phase having two relaxation mechanisms.

with different natural configurations. The reason for having two natural configurations is that the experimental data suggest that the behavior of the amorphous phase is characterized by two relaxation mechanisms. The deformation gradient $\mathbf{F}_{\kappa_R}$ denotes the mapping between the tangent space associated with κ_R, at the material point to the tangent space associated with $\kappa_{c(t)}$. Also, $\kappa_{p_1(t)}$ and $\kappa_{p_2(t)}$ are the two natural configurations associated with the material, with $\kappa_{p_1(t)}$ associated with the smaller relaxation time and $\kappa_{p_2(t)}$ associated with the larger relaxation time. Also, let $\mathbf{F}_{\kappa_{p_1(t)}}$denote the mapping between the tangent space associated with the configuration $\kappa_{p_1(t)}$, at the material point to the tangent space associated with the current configuration $\kappa_{c(t)}$ and similarly $\mathbf{F}_{\kappa_{p_2(t)}}$ is the mapping between the tangent space associated with the configuration $\kappa_{p_2(t)}$, at the material point to the tangent space associated with the current configuration $\kappa_{c(t)}$. The natural configurations, $\kappa_{p_1(t)}$ and $\kappa_{p_2(t)}$, are not fixed as in an elastic solid but evolve as the material is deformed. We also define $\mathbf{G}_1$ and $\mathbf{G}_2$ to be the mapping between κ_R and the natural configurations $\kappa_{p_1(t)}$ and $\kappa_{p_2(t)}$, respectively, i.e.,

$$\mathbf{G}_i \equiv \mathbf{F}_{\kappa_R \to \kappa_{p_i(t)}} = \mathbf{F}^{-1}_{\kappa_{p_i(t)}} \mathbf{F}_{\kappa_R}, \quad i = 1, 2. \tag{9}$$

We define the velocity gradients, $\mathbf{L}_{\kappa_{p_i(t)}}$, and the symmetric part of $\mathbf{L}_{\kappa_{p_i(t)}}$, $\mathbf{D}_{\kappa_{p_i(t)}}$ to be

$$\mathbf{L}_{\kappa_{p_i(t)}} = \dot{\mathbf{G}}_i \mathbf{G}_i^{-1}, \quad \mathbf{D}_{\kappa_{p_i(t)}} = \tfrac{1}{2}\left(\mathbf{L}_{\kappa_{p_i(t)}} + \mathbf{L}^{\mathrm{T}}_{\kappa_{p_i(t)}}\right), \qquad i = 1, 2. \tag{10}$$

In this approach, the left Cauchy stretch tensors $\mathbf{B}_{\kappa_{p_i(t)}}$ play the role of physically motivated internal variables. It can be easily shown (Rajagopal and Srinivasa, 1999b) that

$$\overset{\nabla}{\mathbf{B}}_{\kappa_{p_i(t)}} := \dot{\mathbf{B}}_{\kappa_{p_i(t)}} - \mathbf{L}\mathbf{B}_{\kappa_{p_i(t)}} - \mathbf{B}_{\kappa_{p_i(t)}}\mathbf{L}^{\mathrm{T}} = -2\mathbf{F}_{\kappa_{p_i(t)}} \mathbf{D}_{\kappa_{p_i(t)}} \mathbf{F}^{\mathrm{T}}_{\kappa_{p_i(t)}}, \quad i = 1, 2, \tag{11}$$

where the inverted triangle denotes the upper convected Oldroyd derivative and the dot is the material time derivative. Specification of $\mathbf{D}_{\kappa_{p_i(t)}}$ is tantamount to prescribing the manner in which the underlying natural configurations change. As the material is incompressible, we shall assume that the motions associated with each of the natural configurations are isochoric, i.e.,

$$\mathrm{tr}\left(\mathbf{D}_{\kappa_{p_i(t)}}\right) = 0, \quad i = 1, 2. \tag{12}$$

We derive forms for $\mathbf{D}_{\kappa_{p_i(t)}}$, $i = 1, 2$, using the second law in the form of the reduced energy-dissipation equation and by requiring that the rate of dissipation be maximized. We make the following constitutive assumptions on the Helmholtz potential,

$$\psi_a = \psi_a\left(\mathbf{B}_{\kappa_{p_1(t)}}, \mathbf{B}_{\kappa_{p_2(t)}}\right), \tag{13}$$

where ψ_a is the Helmholtz potential of amorphous phase. We further assume that the Helmholtz potential associated with the two natural configurations are additive, i.e.,

$$\psi_a = \psi_1\left(\mathbf{B}_{\kappa_{p_1(t)}}\right) + \psi_2\left(\mathbf{B}_{\kappa_{p_2(t)}}\right) + E_a, \tag{14}$$

where E_a is the thermal contribution to the Helmholtz potential and is a constant for this problem. Since amorphous PET is isotropic, the forms for ψ_1 and ψ_2 are those of an isotropic material and have the following forms:

$$\psi_i = \psi_i(\mathrm{I}_i, \mathrm{II}_i), \quad i = 1, 2, \tag{15}$$

where

$$\mathrm{I}_i = \mathrm{tr}\left(\mathbf{B}_{\kappa_{p_i(t)}}\right), \quad \mathrm{II}_i = \mathrm{tr}\left(\mathbf{B}^2_{\kappa_{p_i(t)}}\right), \qquad i = 1, 2. \tag{16}$$

Since the material is isotropic, we can choose without any loss of generality configurations $\kappa_{\mathrm{p}_1(t)}$ and $\kappa_{\mathrm{p}_2(t)}$ appropriately rotated such that

$$\mathbf{F}_{\kappa_{\mathrm{p}_i(t)}} = \mathbf{V}_{\kappa_{\mathrm{p}_i(t)}}, \quad i = 1, 2, \tag{17}$$

where $\mathbf{V}_{\kappa_{\mathrm{p}_i(t)}}$, $i = 1, 2$, are the right stretch tensors in the polar decomposition. We assume the following form for the rate of dissipation:

$$\zeta = \zeta_1\left(\mathbf{B}_{\kappa_{\mathrm{p}_1(t)}}, \mathbf{D}_{\kappa_{\mathrm{p}_1(t)}}\right) + \zeta_2\left(\mathbf{B}_{\kappa_{\mathrm{p}_2(t)}}, \mathbf{D}_{\kappa_{\mathrm{p}_2(t)}}\right) \tag{18}$$

with the additional assumption that the rate of dissipation associated with a natural configuration is zero when it is not changing, i.e.,

$$\zeta_i\left(\mathbf{B}_{\kappa_{\mathrm{p}_i(t)}}, \mathbf{0}\right) = 0, \quad i = 1, 2. \tag{19}$$

We also assume that the rate dissipation associated with each natural configuration is non-negative, i.e.,

$$\zeta_i \geqslant 0, \quad i = 1, 2. \tag{20}$$

Substituting Eqs. (15) and (11) into Eq. (8) and using Eq. (17), we get

$$\left(\mathbf{T} - \sum_{i=1}^{2} 2\rho\left[\frac{\partial \psi_i}{\partial \mathrm{I}_i}\mathbf{B}_{\kappa_{\mathrm{p}_i(t)}} + 2\frac{\partial \psi_i}{\partial \mathrm{II}_i}\mathbf{B}^2_{\kappa_{\mathrm{p}_i(t)}}\right]\right) \cdot \mathbf{D} + \sum_{i=1}^{2}\left(2\rho\left[\frac{\partial \psi_i}{\partial \mathrm{I}_i}\mathbf{B}_{\kappa_{\mathrm{p}_i(t)}} + 2\frac{\partial \psi_i}{\partial \mathrm{II}_i}\mathbf{B}^2_{\kappa_{\mathrm{p}_i(t)}}\right] \cdot \mathbf{D}_{\kappa_{\mathrm{p}_i(t)}}\right)$$
$$= \sum_{i=1}^{2}\zeta_i\left(\mathbf{B}_{\kappa_{\mathrm{p}_i(t)}}, \mathbf{D}_{\kappa_{\mathrm{p}_i(t)}}\right) \geqslant 0. \tag{21}$$

Since the second term of Eq. (21) and the right-hand side are independent of $\mathbf{D}$ and noting that only isochoric motions are permissible, it is sufficient to assume the stress has the form

$$\mathbf{T} = -p\mathbf{I} + \sum_{i=1}^{2} 2\rho\left[\frac{\partial \psi_i}{\partial \mathrm{I}_i}\mathbf{B}_{\kappa_{\mathrm{p}_i(t)}} + 2\frac{\partial \psi_i}{\partial \mathrm{II}_i}\mathbf{B}^2_{\kappa_{\mathrm{p}_i(t)}}\right]. \tag{22}$$

This assumption is sufficient to ensure that for all motions for which the natural configurations do not change, the material responds elastically. We also define the partial extra stresses associated with each of the natural configurations

$$\mathbf{T}_i = 2\rho\left[\frac{\partial \psi_i}{\partial \mathrm{I}_i}\mathbf{B}_{\kappa_{\mathrm{p}_i(t)}} + 2\frac{\partial \psi_i}{\partial \mathrm{II}_i}\mathbf{B}^2_{\kappa_{\mathrm{p}_i(t)}}\right], \quad i = 1, 2. \tag{23}$$

Using Eqs. (22) and (23), Eq. (21) reduces to

$$\mathbf{T}_1 \cdot \mathbf{D}_{\kappa_{\mathrm{p}_1(t)}} + \mathbf{T}_2 \cdot \mathbf{D}_{\kappa_{\mathrm{p}_2(t)}} = \zeta_1 + \zeta_2. \tag{24}$$

From the forms chosen for the Helmholtz potential and the rate of dissipation, it is clear that

$$\mathbf{T}_i \cdot \mathbf{D}_{\kappa_{\mathrm{p}_i(t)}} = \zeta_i, \quad i = 1, 2. \tag{25}$$

Eq. (25) places restrictions on the tensors $\mathbf{D}_{\kappa_{\mathrm{p}_i(t)}}$ that are achievable. We assume (similar to Rajagopal and Srinivasa (2000)) that the actual value of $\mathbf{D}_{\kappa_{\mathrm{p}_i(t)}}$, $i = 1, 2$, chosen satisfies the constraints given by Eqs. (25) and (12) and also corresponds to a maximum for the rate of dissipation. This is enforced using the method of Lagrange multipliers by extremizing Eq. (18) subject to the constraints (25) and (12). On doing this, we obtain the following equations for the determination of $\mathbf{D}_{\kappa_{\mathrm{p}_i(t)}}$,

$$\mathbf{T}_i - \beta_{1i}\frac{\partial \zeta_i}{\partial \mathbf{D}_{\kappa_{\mathrm{p}_i(t)}}} - \beta_{2i}\mathbf{I} = \mathbf{0}, \quad i = 1,2, \tag{26}$$

where β_{1i} and β_{2i} are Lagrange multipliers.

For the problem under consideration, we assume that the Helmholtz potential associated with the elastic response of the amorphous phase is that of a neo-Hookean material, i.e.,

$$\psi_i = \frac{\mu_i}{2\rho}(I_i - 3), \quad i = 1,2. \tag{27}$$

We also assume that the rate of dissipation has the form

$$\zeta_i = 2\eta_i \mathbf{D}_{\kappa_{\mathrm{p}_i(t)}} \cdot \mathbf{B}_{\kappa_{\mathrm{p}_i(t)}} \mathbf{D}_{\kappa_{\mathrm{p}_i(t)}}, \quad i = 1,2, \tag{28}$$

where the material constant μ_i is the elastic modulus and the material function η_i is the viscosity of the material, which we assume can depend on $\mathbf{B}_{\kappa_{\mathrm{p}_i(t)}}$. With these assumptions, Eq. (22) reduces to

$$\mathbf{T} = -p\mathbf{I} + \mu_1 \mathbf{B}_{\kappa_{\mathrm{p}_1(t)}} + \mu_2 \mathbf{B}_{\kappa_{\mathrm{p}_2(t)}}, \tag{29}$$

and Eq. (23) reduces to

$$\mathbf{T}_i = \mu_i \mathbf{B}_{\kappa_{\mathrm{p}_i(t)}}, \quad i = 1,2. \tag{30}$$

Substituting Eq. (28) into Eq. (26) and eliminating β_{1i} by using Eqs. (12) and (25), we obtain

$$\mathbf{T}_i = 2\eta_i \mathbf{B}_{\kappa_{\mathrm{p}_i(t)}} \mathbf{D}_{\kappa_{\mathrm{p}_i(t)}} + \beta_{2i}\mathbf{I}, \quad i = 1,2. \tag{31}$$

From Eqs. (30), (31), (11), (12) and (17), we obtain

$$\overset{\nabla}{\mathbf{B}}_{\kappa_{\mathrm{p}_i(t)}} := \dot{\mathbf{B}}_{\kappa_{\mathrm{p}_i(t)}} - \mathbf{L}\mathbf{B}_{\kappa_{\mathrm{p}_i(t)}} - \mathbf{B}_{\kappa_{\mathrm{p}_i(t)}}\mathbf{L}^{\mathrm{T}} = \frac{\mu_i}{\eta_i}\left(\frac{3}{\mathrm{tr}(\mathbf{B}^{-1}_{\kappa_{\mathrm{p}_i(t)}})}\mathbf{I} - \mathbf{B}_{\kappa_{\mathrm{p}_i(t)}}\right), \quad i = 1,2. \tag{32}$$

The specific form for the viscosity function that we use in this work is given by

$$\eta_1 = \bar{\eta}_1\left(N\left(\mathrm{tr}\left(\mathbf{B}_{\kappa_{\mathrm{p}_1(t)}}\right) - 3\right)^m + 1\right), \tag{33}$$

$$\eta_2 = \bar{\eta}_2, \tag{34}$$

where $\bar{\eta}_1$, $\bar{\eta}_2$, N and m are constants. Also, the relaxation times associated with the two natural configurations are given by

$$\lambda_i = \frac{\eta_i}{\mu_i}, \quad i = 1,2. \tag{35}$$

This completes the development of the model for the amorphous phase.

4. Modeling of semi-crystalline mixture

When PET is deformed at temperatures just above the glass transition temperature, crystallization takes place, and the new material is a mixture of an amorphous phase and crystalline phase. Crystallization does not all take place at an instant but generally takes place in a gradual manner. In order to model this, we have to make constitutive assumptions for this mixed region.

We treat the mixture of the crystalline and amorphous phases as a constrained mixture. We allow co-occupancy of the phases in an averaged sense as is done in traditional mixture theory (Truesdell, 1957; Bowen, 1975; Atkin and Craine, 1976; Rajagopal and Tao, 1995). We also assume that the amorphous and

crystalline components are constrained to move together, which for polymers is a reasonable assumption as the same molecule traverses both the amorphous and crystalline phases.

The newly formed crystalline material is assumed to be an elastic solid. For elastic solids, the stress depends on the deformation gradient from a configuration of known stress (usually a stress free configuration) and its current configuration. Here we assume that the crystalline material is born in a stress-free state. This is similar to the approach used by Rajagopal and Wineman (1992) for their multi-network theory for polymers. It is well known that when strain-induced crystallization takes place in polymers, the crystals that are formed are oriented. The formation of oriented crystals results in anisotropy in the mechanical response of the material. This anisotropy in the mechanical response is included in the model by choosing the Helmholtz potential for the newly formed crystalline material to be that of an anisotropic elastic solid. The anisotropy of the elastic solid is determined by the deformation in the amorphous phase at the instant of formation of the crystalline phase. Anisotropy is induced in the crystalline phase in the same manner as was done by Rao and Rajagopal (2000). The main difference being that in the previous paper, the amorphous phase had a single relaxation mechanism associated with it. Here the amorphous phase has two relaxation mechanisms associated with it. We use the tensor $\mathbf{B}_{\kappa_{\mathrm{p}_2(\tau)}}$ to reflect the induced anisotropy in the crystalline phase formed at the instant $t=\tau$. This tensor is associated with the natural configuration having the larger relaxation time. Also, the tensor $\mathbf{B}_{\kappa_{\mathrm{p}_2(\tau)}}$ contains information about the orientation of the molecules in the amorphous phase, albeit in an averaged way. Just as in Rao and Rajagopal (2000), we use the principal directions of $\mathbf{B}_{\kappa_{\mathrm{p}_2(\tau)}}$ to determine the anisotropy in the crystalline phase and further assume that the anisotropy of the newly formed crystalline material at each instant is orthotropic. With these assumptions, the Helmholtz potential of the crystalline phase born is given by

$$\psi_{\mathrm{c}} = \psi_{\mathrm{c}}(I_{\mathrm{c}_1}, I_{\mathrm{c}_2}, J_1, J_2, K_1, K_2), \tag{36}$$

where I_{c_1} and I_{c_2} are the first two invariants of the right Cauchy–Green stretch tensor, $\mathbf{C}_{\kappa_{\mathrm{c}(\tau)}}$ and the following scalars:

$$\begin{aligned} J_1 &= \mathbf{n}_{\kappa_{\mathrm{c}(\tau)}} \cdot \mathbf{C}_{\kappa_{\mathrm{c}(\tau)}} \mathbf{n}_{\kappa_{\mathrm{c}(\tau)}}, \quad K_1 = \mathbf{m}_{\kappa_{\mathrm{c}(\tau)}} \cdot \mathbf{C}_{\kappa_{\mathrm{c}(\tau)}} \mathbf{m}_{\kappa_{\mathrm{c}(\tau)}}, \\ J_2 &= \mathbf{n}_{\kappa_{\mathrm{c}(\tau)}} \cdot \mathbf{C}^2_{\kappa_{\mathrm{c}(\tau)}} \mathbf{n}_{\kappa_{\mathrm{c}(\tau)}}, \quad K_2 = \mathbf{m}_{\kappa_{\mathrm{c}(\tau)}} \cdot \mathbf{C}^2_{\kappa_{\mathrm{c}(\tau)}} \mathbf{m}_{\kappa_{\mathrm{c}(\tau)}}, \end{aligned} \tag{37}$$

where $\mathbf{n}_{\kappa_{\mathrm{c}(\tau)}}$ and $\mathbf{m}_{\kappa_{\mathrm{c}(\tau)}}$ are two eigenvectors of the tensor $\mathbf{B}_{\kappa_{\mathrm{p}_2(\tau)}}$ which determine the anisotropy of the crystals that are formed. The configuration $\kappa_{\mathrm{c}(\tau)}$ is the configuration occupied by the body at time $t=\tau$. This is the stress-free configuration for the crystalline material born at time $t=\tau$. This is illustrated in Fig. 3, where the tensor $\mathbf{F}_{\kappa_{\mathrm{c}(\tau)}}$ is the mapping between the tangent spaces of configurations $\kappa_{\mathrm{c}(\tau)}$ and the current configuration $\kappa_{\mathrm{c}(t)}$. Since the configuration $\kappa_{\mathrm{c}(\tau)}$ is the stress-free configuration of the crystalline material born at time $t=\tau$, the Helmholtz potential depends on $\mathbf{F}_{\kappa_{\mathrm{c}(\tau)}}$ through $\mathbf{C}_{\kappa_{\mathrm{c}(\tau)}}$. The specific form of the Helmholtz potential used here is

$$\psi_{\mathrm{c}} = \frac{1}{2\rho}\left(\mu_{\mathrm{c}}(I_{\mathrm{c}_1}-3) + \mu_{\mathrm{c}_1}(J_1-1)^2 + \mu_{\mathrm{c}_2}(K_1-1)^2\right) + E_{\mathrm{c}}, \tag{38}$$

where E_{c} is the thermal contribution to the Helmholtz potential, the material moduli μ_{c}, μ_{c_1} and μ_{c_2} can depend on the conditions in the amorphous phase at the instant of formation through the appropriate invariants of $\mathbf{B}_{\kappa_{\mathrm{p}_1(\tau)}}$ and $\mathbf{B}_{\kappa_{\mathrm{p}_2(\tau)}}$. We expect the value of the material moduli to be larger when the crystalline material is formed from an amorphous phase that is extended, i.e., the greater the stretch in the amorphous phase, the greater the value of the moduli of the newly formed crystalline phase. The specific forms chosen are

$$\begin{aligned} &\mu_{\mathrm{c}} = \bar{\mu}_{\mathrm{c}}(\mu_1(I_1-3) + \mu_2(I_2-3) - F), \qquad \mu_{\mathrm{c}_1} = \bar{\mu}_{\mathrm{c}_1}(\mu_1(I_1-3) + \mu_2(I_2-3) - F), \\ &\mu_{\mathrm{c}_2} = \bar{\mu}_{\mathrm{c}_2}(\mu_1(I_1-3) + \mu_2(I_2-3) - F), \end{aligned} \tag{39}$$

where I_1 and I_2 are evaluated at the instant of crystallization and $\bar{\mu}_{\mathrm{c}}$, $\bar{\mu}_{\mathrm{c}_1}$, $\bar{\mu}_{\mathrm{c}_2}$ and F are constant.

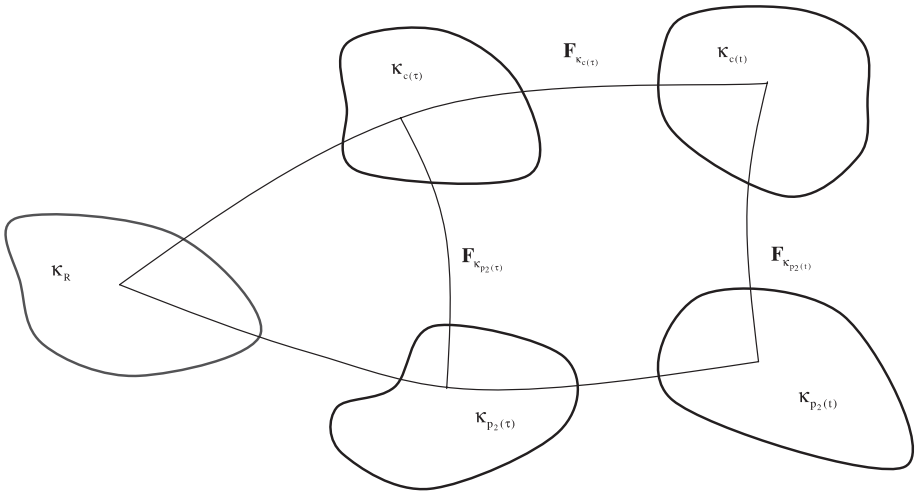

Fig. 3. Natural configurations associated with the amorphous–crystalline mixture.

The Helmholtz potential for the mixture is assumed to be additive, i.e.,

$$\psi = \int_{\tau_s}^{t} \psi_c \frac{d\alpha}{d\tau} d\tau + (1-\alpha)\psi_a, \tag{40}$$

where τ_s is the time at which crystallization begins, α is the mass fraction of the crystalline phase and ψ_c and ψ_a are given by Eqs. (38) and (14), respectively. In Eq. (40), there is an integral as the crystalline phase is formed gradually and not at an instant.

The formation of the crystalline phase also affects the response of the amorphous phase. The formation of the crystalline phase reduces the mobility of the molecules in the amorphous phase as the molecules are pinned down. This manifests itself at the macroscopic level as an increase in the relaxation time of the amorphous phase. We model this by making the viscosity of the amorphous phase a function of the mass fraction of the crystalline phase. The specific forms chosen are

$$\eta_1 = \bar{\eta}_1 \left(N \left(\mathrm{tr} \left(\mathbf{B}_{\kappa_{p_1(t)}} \right) - 3 \right)^m + 1 \right) \exp(L_1 \alpha), \tag{41}$$

$$\eta_2 = \bar{\eta}_2 \exp(L_2 \alpha), \tag{42}$$

where L_1, L_2, N and m are constants with N and m the same as in Eq. (33). Note that Eqs. (41) and (42) reduce to the forms in Eqs. (33) and (34) for zero crystallinity. The rate of dissipation in the amorphous part after crystallization has begun is assumed to be given by

$$\zeta_i = (1-\alpha) 2\eta_i \mathbf{D}_{\kappa_{p_i(t)}} \cdot \mathbf{B}_{\kappa_{p_i(t)}} \mathbf{D}_{\kappa_{p_i(t)}}, \quad i = 1, 2. \tag{43}$$

The above form is different from Eq. (28) for a pure amorphous phase in that the rate of dissipation is proportional to the amount of amorphous phase remaining and Eq. (43) reduces to Eq. (28) for zero crystallinity.

Crystallization in polymers is in general an irreversible process, i.e., entropy production takes place during crystallization. The rate of dissipation which depends on the amount of crystallinity (α), the rate of change of crystallinity ($\dot{\alpha}$) and can in general depend on other variables as well, i.e.,

$$\zeta_c = \zeta_c(\alpha, \dot{\alpha}, \ldots). \tag{44}$$

The rate of dissipation in Eq. (44) has to be exactly zero when no crystallization takes place, i.e.,

$$\zeta_{\mathrm{c}}|_{\dot{\alpha}=0} = 0. \tag{45}$$

We also assume that the rate of dissipation due to crystallization is non-negative, i.e.,

$$\zeta_{\mathrm{c}} \geqslant 0. \tag{46}$$

Thus, we choose the following form that satisfies Eqs. (45) and (46),

$$\zeta_{\mathrm{c}} = (A + B\alpha)\dot{\alpha}, \tag{47}$$

where A and B are constants. Eq. (47) is valid for a crystallizing system, i.e., $\dot{\alpha} \geqslant 0$, if melting of crystals takes place, a separate equation will have to be prescribed for that case. The total rate of dissipation after crystallization has been initiated is given by

$$\zeta = (1-\alpha)\left(2\eta_1 \mathbf{D}_{\kappa_{\mathrm{p}_1(t)}} \cdot \mathbf{B}_{\kappa_{\mathrm{p}_1(t)}} \mathbf{D}_{\kappa_{\mathrm{p}_1(t)}} + 2\eta_2 \mathbf{D}_{\kappa_{\mathrm{p}_2(t)}} \cdot \mathbf{B}_{\kappa_{\mathrm{p}_2(t)}} \mathbf{D}_{\kappa_{\mathrm{p}_2(t)}}\right) + (A + B\alpha)\dot{\alpha}. \tag{48}$$

Substituting Eqs. (40) and (48) into Eq. (8), and using Eq. (11) we get

$$\begin{aligned}
&\left(\mathbf{T} - (1-\alpha)\sum_{i=1}^{2} 2\rho\left[\frac{\partial \psi_i}{\partial \mathrm{I}_i}\mathbf{B}_{\kappa_{\mathrm{p}_i(t)}} + 2\frac{\partial \psi_i}{\partial \mathrm{II}_i}\mathbf{B}^2_{\kappa_{\mathrm{p}_i(t)}}\right] - 2\rho\left[\int_{\tau_{\mathrm{s}}}^{t} \mathbf{F}_{\kappa_{\mathrm{c}(\tau)}} \frac{\partial \psi_{\mathrm{c}}}{\partial \mathbf{C}_{\kappa_{\mathrm{c}(\tau)}}} \mathbf{F}^{\mathrm{T}}_{\kappa_{\mathrm{c}(\tau)}} \frac{\mathrm{d}\alpha}{\mathrm{d}\tau}\mathrm{d}\tau\right]\right) \cdot \mathbf{D} \\
&\quad + (1-\alpha)\sum_{i=1}^{2}\left(2\rho\left[\frac{\partial \psi_i}{\partial \mathrm{I}_i}\mathbf{B}_{\kappa_{\mathrm{p}_i(t)}} + 2\frac{\partial \psi_i}{\partial \mathrm{II}_i}\mathbf{B}^2_{\kappa_{\mathrm{p}_i(t)}}\right] \cdot \mathbf{D}_{\kappa_{\mathrm{p}_i(t)}}\right) + \rho\left(\psi_{\mathrm{a}} - \psi_{\mathrm{c}}|_{\mathbf{C}_{\kappa_{\mathrm{c}(\tau)}}=\mathbf{I}}\right)\dot{\alpha} \\
&\quad = (1-\alpha)\left(2\eta_1 \mathbf{D}_{\kappa_{\mathrm{p}_1(t)}} \cdot \mathbf{B}_{\kappa_{\mathrm{p}_1(t)}} \mathbf{D}_{\kappa_{\mathrm{p}_1(t)}} + 2\eta_2 \mathbf{D}_{\kappa_{\mathrm{p}_2(t)}} \cdot \mathbf{B}_{\kappa_{\mathrm{p}_2(t)}} \mathbf{D}_{\kappa_{\mathrm{p}_2(t)}}\right) + (A + B\alpha)\dot{\alpha}.
\end{aligned} \tag{49}$$

The above equation gives us guidance for the forms to choose for the stress tensor. The following form is sufficient to satisfy the above inequality:

$$\mathbf{T} = -p\mathbf{I} + (1-\alpha)\sum_{i=1}^{2} 2\rho\left[\frac{\partial \psi_i}{\partial \mathrm{I}_i}\mathbf{B}_{\kappa_{\mathrm{p}_i(t)}} + 2\frac{\partial \psi_i}{\partial \mathrm{II}_i}\mathbf{B}^2_{\kappa_{\mathrm{p}_i(t)}}\right] + 2\rho\left[\int_{\tau_s}^{t} \mathbf{F}_{\kappa_{\mathrm{c}(\tau)}} \frac{\partial \psi_{\mathrm{c}}}{\partial \mathbf{C}_{\kappa_{\mathrm{c}(\tau)}}} \mathbf{F}^{\mathrm{T}}_{\kappa_{\mathrm{c}(\tau)}} \frac{\mathrm{d}\alpha}{\mathrm{d}\tau}\mathrm{d}\tau\right]. \tag{50}$$

Defining the partial stresses associated with the two relaxation mechanisms of the amorphous phase as

$$\mathbf{T}_i = 2(1-\alpha)\rho\left[\frac{\partial \psi_i}{\partial \mathrm{I}_i}\mathbf{B}_{\kappa_{\mathrm{p}_i(t)}} + 2\frac{\partial \psi_i}{\partial \mathrm{II}_i}\mathbf{B}^2_{\kappa_{\mathrm{p}_i(t)}}\right], \quad i = 1, 2, \tag{51}$$

and the partial stress associated with the crystalline phase is

$$\mathbf{T}_{\mathrm{c}} = 2\rho\left[\int_{\tau_{\mathrm{s}}}^{t} \mathbf{F}_{\kappa_{\mathrm{c}(\tau)}} \frac{\partial \psi_{\mathrm{c}}}{\partial \mathbf{C}_{\kappa_{\mathrm{c}(\tau)}}} \mathbf{F}^{\mathrm{T}}_{\kappa_{\mathrm{c}(\tau)}} \frac{\mathrm{d}\alpha}{\mathrm{d}\tau}\mathrm{d}\tau\right]. \tag{52}$$

For the specific forms chosen for the Helmholtz potentials (Eqs. (27) and (38)), the stress reduces to

$$\begin{aligned}
\mathbf{T} = -p\mathbf{I} + (1-\alpha)\left(\mu_1 \mathbf{B}_{\kappa_{\mathrm{p}_1(t)}} + \mu_2 \mathbf{B}_{\kappa_{\mathrm{p}_2(t)}}\right) + \int_{\tau_{\mathrm{s}}}^{t} \mu_{\mathrm{c}} \mathbf{B}_{\kappa_{\mathrm{c}(\tau)}} \frac{\mathrm{d}\alpha}{\mathrm{d}\tau}\mathrm{d}\tau + 2\int_{\tau_{\mathrm{s}}}^{t}\Big(\mathbf{F}_{\kappa_{\mathrm{c}(\tau)}}\Big(\mu_{\mathrm{c}1}(J_1 - 1)\mathbf{n}_{\kappa_{\mathrm{c}(\tau)}} \otimes \mathbf{n}_{\kappa_{\mathrm{c}(\tau)}} \\
+ \mu_{\mathrm{c}2}(K_1 - 1)\mathbf{m}_{\kappa_{\mathrm{c}(\tau)}} \otimes \mathbf{m}_{\kappa_{\mathrm{c}(\tau)}}\Big)\mathbf{F}^{\mathrm{T}}_{\kappa_{\mathrm{c}(\tau)}}\Big)\frac{\mathrm{d}\alpha}{\mathrm{d}\tau}\mathrm{d}\tau.
\end{aligned} \tag{53}$$

Using Eqs. (50) and (51) in Eq. (49), we get

$$\mathbf{T}_1 \cdot \mathbf{D}_{\kappa_{\mathrm{p}_1(t)}} + \mathbf{T}_2 \cdot \mathbf{D}_{\kappa_{\mathrm{p}_2(t)}} + \rho\left(\psi_{\mathrm{a}} - \psi_{\mathrm{c}}|_{\mathbf{C}_{\kappa_{\mathrm{c}(\tau)}}=\mathbf{I}}\right)\dot{\alpha} = (1-\alpha)\Big(2\eta_1 \mathbf{D}_{\kappa_{\mathrm{p}_1(t)}} \cdot \mathbf{B}_{\kappa_{\mathrm{p}_1(t)}} \mathbf{D}_{\kappa_{\mathrm{p}_1(t)}} + 2\eta_2 \mathbf{D}_{\kappa_{\mathrm{p}_2(t)}} \cdot \mathbf{B}_{\kappa_{\mathrm{p}_2(t)}} \mathbf{D}_{\kappa_{\mathrm{p}_2(t)}}\Big) + (A + B\alpha)\dot{\alpha}. \tag{54}$$

We further assume that the different modes of the rate of dissipation are independent, this results in the following relationships:

$$\mathbf{T}_i \cdot \mathbf{D}_{\kappa i_{\mathrm{p}(t)}} = (1-\alpha)\Big(2\eta_i \mathbf{D}_{\kappa_{\mathrm{p}_i(t)}} \cdot \mathbf{B}_{\kappa_{\mathrm{p}_i(t)}} \mathbf{D}_{\kappa_{\mathrm{p}_i(t)}}\Big), \quad i = 1,2, \tag{55}$$

$$\rho\left(\psi_{\mathrm{a}} - \psi_{\mathrm{c}}|_{\mathbf{C}_{\kappa_{\mathrm{c}(\tau)}}=\mathbf{I}}\right)\dot{\alpha} = (A + B\alpha)\dot{\alpha}. \tag{56}$$

Extremizing the rate of dissipation, Eq. (48), subject to the constraints, Eqs. (55) and (56) results in rate equations for $\mathbf{B}_{\kappa_{\mathrm{p}_i(t)}}$, $i = 1,2$, given by Eq. (32). However, note that after crystallization has been initiated, Eq. (32) is different from the equation prior to crystallization as the viscosities η_1 and η_2 are given by Eqs. (41) and (42) instead of Eqs. (33) and (34). Consequently, the relaxation times are different, their values also depending on the value of crystallinity.

The rate at which crystallization takes place can be derived from Eq. (56). When no crystallization takes place, $\dot{\alpha} = 0$, Eq. (56) is automatically satisfied. However, when crystallization takes place, i.e. $\dot{\alpha} \neq 0$, Eq. (56) is satisfied only if

$$\rho\left(\psi_{\mathrm{a}} - \psi_{\mathrm{c}}|_{\mathbf{C}_{\kappa_{\mathrm{c}(\tau)}}=\mathbf{I}}\right) = A + B\alpha. \tag{57}$$

Substituting Eqs. (38), (14) and (27) into the above equation and noting that

$$\psi_{\mathrm{c}}|_{\mathbf{C}_{\kappa_{\mathrm{c}(\tau)}}=\mathbf{I}} = E_{\mathrm{c}}, \tag{58}$$

because the crystalline solid is born in a stress-free state, we get

$$\frac{u_1}{2}\left(\mathrm{tr}\left(\mathbf{B}_{\kappa_{\mathrm{p}_1(t)}}\right) - 3\right) + \frac{u_2}{2}\left(\mathrm{tr}\left(\mathbf{B}_{\kappa_{\mathrm{p}_2(t)}}\right) - 3\right) + \rho(E_{\mathrm{a}} - E_{\mathrm{c}}) = A + B\alpha, \tag{59}$$

where A and B are constants. The above equation gives the amount of crystalline material formed and can be converted to a crystallization rate by differentiating with respect to time. In Eq. (59), the constant A is related to the initiation of crystallization. At the instant crystallization is initiated, the value of crystallinity is zero; however, the rate of crystallization is non-zero, i.e.,

$$\alpha = 0, \quad \dot{\alpha} \neq 0. \tag{60}$$

At this instant, Eq. (59) has to be satisfied. On substituting Eq. (60) into Eq. (59), we get

$$A = \frac{u_1}{2}\left(\mathrm{tr}\left(\mathbf{B}^0_{\kappa_{\mathrm{p}_1(t)}}\right) - 3\right) + \frac{u_2}{2}\left(\mathrm{tr}\left(\mathbf{B}^0_{\kappa_{\mathrm{p}_2(t)}}\right) - 3\right) + \rho(E_{\mathrm{a}} - E_{\mathrm{c}}) = \rho\left(\psi^0_{\mathrm{a}} - E_{\mathrm{c}}\right), \tag{61}$$

where $\mathbf{B}^0_{\kappa_{\mathrm{p}_1(t)}}$ and $\mathbf{B}^0_{\kappa_{\mathrm{p}_2(t)}}$ are the values of $\mathbf{B}_{\kappa_{\mathrm{p}_1(t)}}$ and $\mathbf{B}_{\kappa_{\mathrm{p}_2(t)}}$, respectively, at the instant crystallization is initiated and ψ^0_{a} is the Helmholtz potential at the instant crystallization is initiated. The activation criterion is specified by prescribing a value for $\overline{A}$, which is defined as

$$\overline{A} = \mu_1\left(\mathrm{tr}\left(\mathbf{B}^0_{\kappa_{\mathrm{p}_1(t)}}\right) - 3\right) + \mu_2\left(\mathrm{tr}\left(\mathbf{B}^0_{\kappa_{\mathrm{p}_2(t)}}\right) - 3\right) = 2\rho\left(\psi^0_{\mathrm{a}} - E_{\mathrm{a}}\right) = 2[A - \rho(E_{\mathrm{a}} - E_{\mathrm{c}})]. \tag{62}$$

When $\mathbf{B}_{\kappa_{\mathrm{p}_1(t)}}$ and $\mathbf{B}_{\kappa_{\mathrm{p}_2(t)}}$ take on values such that Eq. (62) is satisfied, crystallization is initiated. Substituting Eq. (62) into Eq. (59), we get

$$\begin{aligned}\alpha &= \frac{1}{B}\left(\mu_1 \mathrm{tr}\left(\mathbf{B}_{\kappa_{\mathrm{p}_1}(t)}\right) + \mu_2 \mathrm{tr}\left(\mathbf{B}_{\kappa_{\mathrm{p}_2}(t)}\right) - \mu_1 \mathrm{tr}\left(\mathbf{B}^0_{\kappa_{\mathrm{p}_1}(t)}\right) - \mu_2 \mathrm{tr}\left(\mathbf{B}^0_{\kappa_{\mathrm{p}_2}(t)}\right)\right) \\ &= \frac{1}{2B}\left(\mu_1 \mathrm{tr}\left(\mathbf{B}_{\kappa_{\mathrm{p}_1}(t)}\right)^{-3} + \mu_2 \mathrm{tr}\left(\mathbf{B}_{\kappa_{\mathrm{p}_2}(t)}\right)^{-3} - \overline{A}\right). \end{aligned} \tag{63}$$

Eq. (63) gives the crystallinity of the material as it is being deformed. This completes the development of the model.

5. Application to film stretching

In the following sections, we shall study two deformations, both of which are constant width extensions. For a constant width extension, as the name suggests, the width of the film is kept constant as it is being extended. This is shown schematically in Fig. 4. If we assume that the deformation is homogeneous, the kinematics of deformation are

$$x = \Lambda(t)X, \quad y = \frac{1}{\Lambda(t)}Y, \quad z = Z, \tag{64}$$

where X, Y and Z are the co-ordinates in the undeformed configuration, x, y and z are the coordinates in the deformed state and $\Lambda(t)$ is the stretch in the direction of extension. The velocity gradient for this motion is given by

$$\mathbf{L} = \mathrm{diag}\left(\frac{\dot{\Lambda}}{\Lambda}, -\frac{\dot{\Lambda}}{\Lambda}, 0\right). \tag{65}$$

The velocity gradient, $\mathbf{L}$, is diagonal, and therefore, the symmetric part of the velocity gradient, $\mathbf{D}$, is the same as $\mathbf{L}$. Also, all the other kinematic tensors, namely $\mathbf{B}_{\kappa_{\mathrm{p}_i(t)}}$, $i = 1, 2$, $\mathbf{F}_{\kappa_{\mathrm{c}(\tau)}}$ and $\mathbf{C}_{\kappa_{\mathrm{c}(\tau)}}$ are also diagonal tensors. $\mathbf{B}_{\kappa_{\mathrm{p}_i(t)}}$, $i = 1, 2$, are obtained by solving Eq. (32). The tensors $\mathbf{F}_{\kappa_{\mathrm{c}(\tau)}}$ and $\mathbf{C}_{\kappa_{\mathrm{c}(\tau)}}$ are

$$\mathbf{F}_{\kappa_{\mathrm{c}(\tau)}} = \mathrm{diag}\left(\frac{\Lambda(t)}{\Lambda(\tau)}, \frac{\Lambda(\tau)}{\Lambda(t)}, 1\right), \tag{66}$$

$$\mathbf{C}_{\kappa_{\mathrm{c}(\tau)}} = \mathrm{diag}\left(\left(\frac{\Lambda(t)}{\Lambda(\tau)}\right)^2, \left(\frac{\Lambda(\tau)}{\Lambda(t)}\right)^2, 1\right). \tag{67}$$

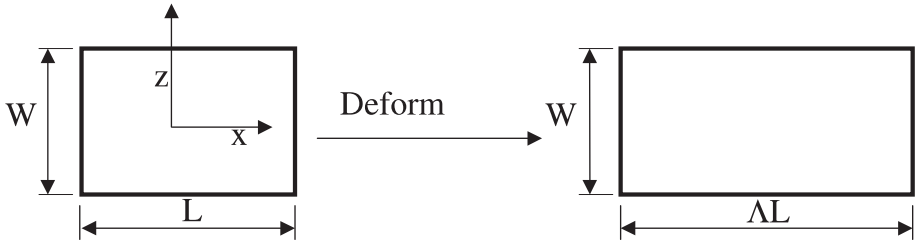

Fig. 4. Schematic of constant width stretching.

For this deformation, the principal directions of $\mathbf{B}_{\kappa_{\mathrm{p}_2(t)}}$ are fixed. We therefore fix the unit vectors $\mathbf{n}_{\kappa_{\mathrm{c}(\tau)}}$ and $\mathbf{m}_{\kappa_{\mathrm{c}(\tau)}}$ to be in the direction of extension and perpendicular to the direction of extension on the plane of the film. Also, if we assume that the lateral surfaces are stress-free, by substituting Eqs. (65)–(67) into Eq. (53) and we obtain

$$T_{11} = (1-\alpha)\left(\mu_1\left(B^1_{11} - B^1_{22}\right) + \mu_2\left(B^2_{11} - B^2_{22}\right)\right) + \int_{\tau_s}^{t}\left(\mu_{\mathrm{c}}\left(\left(\frac{\Lambda(t)}{\Lambda(\tau)}\right)^2 - \left(\frac{\Lambda(\tau)}{\Lambda(t)}\right)^2\right) + 2\mu_{\mathrm{c}_1}\left(\left(\frac{\Lambda(t)}{\Lambda(\tau)}\right)^4 - \left(\frac{\Lambda(t)}{\Lambda(\tau)}\right)^2\right)\right)\frac{\mathrm{d}\alpha}{\mathrm{d}\tau}\mathrm{d}\tau, \tag{68}$$

where B^1_{ij} and B^2_{ij} are the ij components of the tensors $\mathbf{B}_{\kappa_{\mathrm{p}_1(t)}}$ and $\mathbf{B}_{\kappa_{\mathrm{p}_2(t)}}$, respectively. The two modes of deformation studied in this work are the constant extension rate stretching and the constant force stretching.

6. Constant extension rate stretching

This type of stretching is done by clamping the film and extending it at a constant velocity. Experiments have been done on this geometry by Salem (1992, 1998). In this work, the experimental data indicate that the extension rate has a strong effect on the crystallization with crystallization being initiated at smaller extensions for higher extension rates (see data points on Fig. 6). Another significant feature of the experimental results is that there is a rapid increase in the stress after crystallization sets in. We now show that the model developed can predict these two important observations.

For stretching at a constant extension rate, the stretch as a function of time is given by

$$\Lambda(t) = 1 + Kt, \tag{69}$$

where K is a constant. The velocity gradient $\mathbf{L}$ for this motion is given by

$$\mathbf{L} = \mathrm{diag}\left(\frac{K}{1+Kt}, -\frac{K}{1+Kt}, 0\right). \tag{70}$$

The material is initially amorphous in a stress-free state, this corresponds to the following initial conditions for the tensors $\mathbf{B}_{\kappa_{\mathrm{p}_i(t)}}$, $i = 1, 2$,

$$\mathbf{B}_{\kappa_{\mathrm{p}_i(t)}} = \mathbf{I}, \quad \text{for } t = 0. \tag{71}$$

With this initial condition, Eq. (32) is integrated, and the stress in the amorphous regime is given by Eq. (29). When the activation criterion (62) is met, crystallization is initiated. The amount of crystalline fraction is obtained from Eq. (63), and the stress in this regime is given by Eq. (68). This system of equations was integrated using a variable order method for stiff ordinary differential equations. The comparison of the model with experimental data is given in Figs. 5 and 6. Fig. 5 shows the stress versus the extension. The model predicts the rapid increase in stress. Fig. 6 shows the crystallinity versus the stretch, and we see that the model predicts the earlier onset of crystallization for higher rates of extension.

7. Constant force stretching

In this type of stretching, a constant force is applied to the film. The force is held constant, and is related to the stress by

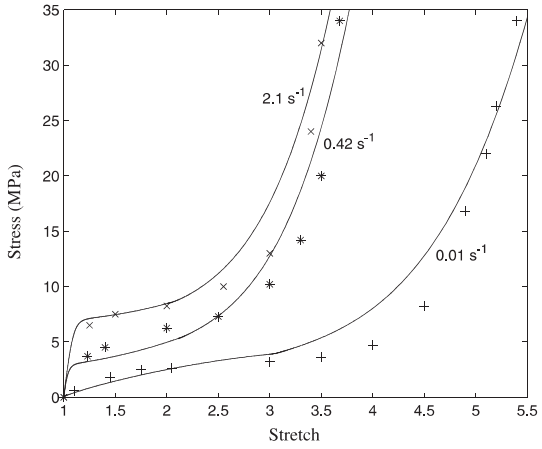

Fig. 5. Plot of stress versus stretch during a constant extension rate drawing for three different rates of extension ($K = 2.1$, 0.42 and 0.01 s^{-1}). The experimental data points ((×) 2.1 s^{-1}, (*) 0.42 s^{-1}, (+) 0.01 s^{-1}) are from Salem (1992). The material constants used are $\mu_1 = 20$ MPa, $\mu_2 = 0.9$ MPa, $\bar{\eta}_1 = 2$ MPa s, $\bar{\eta}_2 = 180$ MPa s, $N = 9$, $m = -4$, $\bar{\mu}_c = 10$ MPa, $\bar{\mu}_{c_1} = 6.5$, $F = 1.4$ MPa, $L_1 = 10$, $L_2 = 1000$, $\overline{A} = 2.4$ MPa and $B = 37$ MPa.

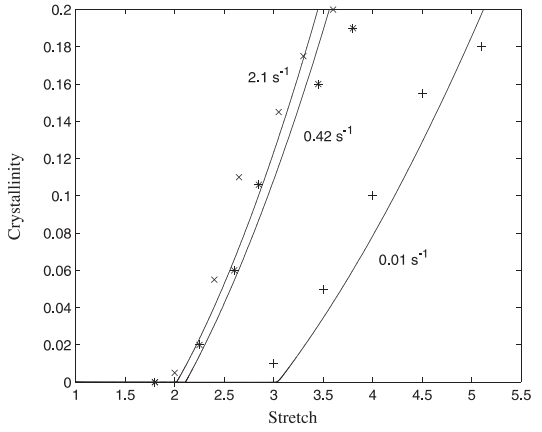

Fig. 6. Plot of crystallinity versus stretch during a constant extension rate drawing at three different rates of extension ($K = 2.1$, 0.42 and 0.01 s^{-1}). The experimental data points ((×) 2.1 s^{-1}, (*) 0.42 s^{-1}, (+) 0.01 s^{-1}) are from Salem (1992). The material constants used are $\mu_1 = 20$ MPa, $\mu_2 = 0.9$ MPa, $\bar{\eta}_1 = 2$ MPa s, $\bar{\eta}_2 = 180$ MPa s, $N = 9$, $m = -4$, $\bar{\mu}_c = 10$ MPa, $\bar{\mu}_{c_1} = 6.5$, $F = 1.4$ MPa, $L_1 = 10$, $L_2 = 1000$, $\overline{A} = 2.4$ MPa and $B = 37$ MPa.

$$F = T_{11}\frac{wh}{\Lambda}, \tag{72}$$

where w is the initial width of the film and h is the initial thickness of the film. We rewrite Eq. (72) as,

$$\sigma_0 = \frac{F}{wh} = \frac{T_{11}}{\Lambda}, \tag{73}$$

where σ_0 is the force per unit initial area and the stress T_{11} is given by Eq. (68). In this problem, the inertial terms are not identically zero as in the case of stretching at a constant extension rate. However, we ignore

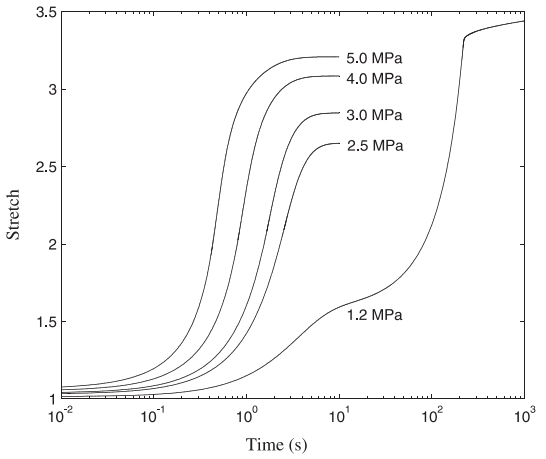

Fig. 7. Plot of stretch versus time during a constant force drawing for different values of force per unit initial area, σ_0. The material constants used are $\mu_1 = 20$ MPa, $\mu_2 = 0.9$ MPa, $\bar{\eta}_1 = 2$ MPa s, $\bar{\eta}_2 = 180$ MPa s, $N = 9$, $m = -4$, $\bar{\mu}_c = 10$ MPa, $\bar{\mu}_{c_1} = 6.5$, $F = 1.4$ MPa, $L_1 = 10$, $L_2 = 1000$, $\overline{A} = 2.4$ MPa and $B = 37$ MPa.

the inertial terms. Eq. (73) is differentiated to furnish a differential equation for Λ which is solved in conjunction with Eq. (32). The initial conditions are obtained by recognizing that on a sudden application of a force, the material reacts initially like an elastic solid with the value of stretch at time $t = 0$, $\Lambda(0)$, given as the solution to the equation

$$T_{11} = \sigma_0 \Lambda = \mu_1 \left(B^1_{11} - B^1_{22}\right) + \mu_2 \left(B^2_{11} - B^2_{22}\right) \tag{74}$$

with

$$B^1_{11} = B^2_{11} = \Lambda(0)^2, \tag{75}$$

$$B^1_{22} = B^2_{22} = \frac{1}{\Lambda(0)^2}. \tag{76}$$

Also, the initial value of B^1_{33} and B^2_{33} is unity. With these initial conditions, the equations are integrated using a variable order method for stiff differential equations. When the activation criterion (62) is met crystallization is initiated. The amount of crystalline fraction is obtained from Eq. (63). The plot of stretch versus time for different values of σ_0 is shown in Fig. 7. In these calculations, we use the same values of material constants as used in the constant extension rate problem. For low values of σ_0 the material flows and reaches a plateau at a much later time. For higher loads, the deformation is more rapid and crystallization is initiated at earlier times. Also, in this regime of rapid deformation, higher loads result in a larger value of plateau stretch. These results are consistent with experimental observations (Bourvellec and Beautemps, 1990a,b).

8. Conclusions

We conclude our study by a very brief recapitulation of the framework that we have used. The model developed here takes into account the fact that materials can exist in stress-free states (modulo rigid body motions) in a variety of configurations. Additionally, it is possible that in these natural configurations, it can possess different material symmetries. Thus, the response of bodies is defined through a set of response

functions from these various natural configurations. As the process proceeds, the underlying natural configuration for the body, and the appropriate response functions change. The choice of the appropriate natural configuration and the associated response function is determined by a thermodynamic criterion, namely the maximization of the rate of dissipation. Choices need to be made for the Helmholtz potential, rate of dissipation and other thermodynamic quantities that characterize the means of storing energy, the manner of dissipation, entropy production due to natural configuration changes, conduction, etc. The study carried out here is a special application of the general framework used to study a variety of dissipative processes (Rajagopal and Wineman, 1992; Rajagopal and Srinivasa, 1995, 1998, 1999, 2000), and is closely related to the work on the multiple response characteristics of certain materials discussed by Rajagopal and Wineman (1980).

Acknowledgements

We thank the Polymer Film Consortium at Texas A&M University and the National Science Foundation for the support of this work.

References

Atkin, R.J., Craine, R.E., 1976. Continuum theory of mixtures: basic theory and historical development. Quarterly Journal of Mechanics and Applied Mathematics 29, 209.

Avrami, M., 1939. Kinetics of phase change. Journal of Chemical Physics 7, 1103.

Baldoni, F., Rajagopal, K.R., 1997. A continuum theory for the thermomechanics of solidification. International Journal of Non-Linear Mechanics 32, 3.

Le Bourvellec, G., Beautemps, J., 1990a. Stretching of PET films under constant load. 1. Kinetics and deformation. Journal of Applied Polymer Science 39, 319.

Le Bourvellec, G., Beautemps, J., 1990b. Stretching of PET films under constant load. 2. Structural analysis. Journal of Applied Polymer Science 39, 329.

Bowen, R.M., 1975. Theory of mixtures. In: Eringen, A.C. (Ed.), Continuum Physics, vol. III. Academic Press, New York.

Buckley, C.P., Jones, D.C., Jones, D.P., 1996. Hot-drawing of poly(ethylene terephthalate) under bi-axial stress: application of a three-dimensional glass–rubber constitutive model. Polymer 37(12), 2403.

Crank, J., 1984. Free and moving boundary problems. Clarendon Press, Oxford.

Eder, G., Janseschitz-Kriegl, H., Liedauer, S., 1990. Crystallization processes in quiescent and moving polymer melts under heat transfer conditions. Progress in Polymer Science 15, 629.

Eder, G., Janseschitz-Kriegl, H., Krobath, G., 1989. Shear induced crystallization, a relaxation phenomenon in melts. Progress in Colloid and Polymer Science 80, 1.

Haas, T.W., Maxwell, B., 1969. Effects of shear stress on the crystallization of linear polyethylene and polybutene-1. Polymer Engineering and Science 9, 225.

Johnson, G.A., Livesay, G.A., Woo, S.L.Y., Rajagopal, K.R., 1996. A single integral finite strain viscoelastic model of ligaments and tendons. Journal of Bioengineering 118 (2), 221.

Katayama, K., Murakami, S., Kobayashi, K., 1976. An apparatus for measuring flow induced crystallization in polymers, vol. 54. Bulletin of the Institute of Chemistry Research, Kyoto University, p. 82.

Kobayashi, K., Nagasawa, T., 1970. Crystallization of sheared polymer melts. Journal of Macromolecular Science (Physics) B4, 331.

Lagasse, R.R., Maxwell, B., 1976. An experimental study of the kinetics of polymer crystallization during shear flow. Polymer Engineering and Science 16, 189.

Landau, L.D., 1967. Collected Papers. Gordon and Breach, New York.

Mackley, M.R., Keller, A., 1973. Flow induced crystallization in polyethylene melts. Polymer 14, 16.

Mackley, M.R., Frank, F.C., Keller, A., 1973. Flow induced crystallization in polyethylene melts. Journal of Material Science 14, 16.

Mandelkern, L., 1964. Crystallization of Polymers. McGraw Hill, New York.

McHugh, A.J., Guy, R.K., Tree, D.A., 1993. Extensional flow-induced crystallization of a polyethylene melt. Colloids and Polymer Science 271, 629.

Nogami, K., Murakami, S., Katayama, K., Kobayashi, K., 1977. An optical study on shear-induced crystallization in polymers, vol. 55. Bulletin of the Institute of Chemistry Research, Kyoto University, p. 277.

Rajagopal, K.R., 1995. Multiple configurations in continuum mechanics, vol. 6. Reports of the Institute for Computational and Applied Mechanics, University of Pittsburgh.

Rajagopal, K.R., Wineman, A.S., 1980. On constitutive equations for branching of response with selectivity. International Journal of Non-Linear Mechanics 15, 83–91.

Rajagopal, K.R., Wineman, A.S., 1992. A constitutive equation for nonlinear solids which undergo deformation induced microstructural changes. International Journal of Plasticity 8, 385.

Rajagopal, K.R., Srinivasa, A.S., 1995. On the inelastic behavior of solids: Part-I – twinning. International Journal of Plasticity 11, 653.

Rajagopal, K.R., Srinivasa, A.S., 1998. Inelastic behavior of materials: Part-I – theoretical underpinnings. International Journal of Plasticity 14, 945.

Rajagopal, K.R., Srinivasa, A.S., 1999. On the thermodynamics of shape memory wires. ZAMP 50, 459–496.

Rajagopal, K.R., Srinivasa, A.S., 2000. A thermodynamic frame-work for rate type fluid models. Journal of Non-Newtonian Fluid Mechanics 2(1), 73–94.

Rajagopal, K.R., Tao, L., 1995. Mechanics of Mixtures. World Scientific, New Jersey.

Rao, I.J., Rajagopal, K.R., 2000. Phenomenological modeling of crystallization in polymers using the notion of multiple natural configurations. Interfaces and Free Boundaries, in press.

Rubinstein, L.I., 1971. The Stefan problem. Translations of mathematics monographs, vol. 27. AMS, Providence, Rhode Island.

Salem, D.R., 1992. Development of crystalline order during hot-drawing of poly(ethylene terephthalate) film: influence of strain rate. Polymer 33(15), 3182.

Salem, D.R., 1998. Microstructure development during constant force drawing of poly(ethylene terephthalate). Polymer 39(26), 7067.

Schultz, J.M., 1991. Theory of crystallization in high-speed spinning. Polymer Engineering Science 31, 661.

Sherwood, C.H., Price, F.P., Stein, R.S., 1978. The effects of shear on the crystallization kinetics of poly(ethylene oxide) and poly (ε-caprolactone) melts. Journal of Polymer Science, Polymer Symposium 63, 77.

Stefan, J., 1891. On the theory of formation of ice, in particular in the polar sea. Annals of Physical Chemistry (Wiedemann) 42, 269.

Truesdell, C., 1957. Sulle Basi Della Thermomeccanica. Rend. Lincei 22, 33.

Ulrich, R.E., Price, F.P., 1976. Morphology development during shearing of poly(ethylene oxide) melts. Journal of Applied Polymer Science 20, 1077.

Wolcowicz, M.D., 1978. Nucleation and crystal growth in sheared poly(1-butene) melts. Journal of Polymer Science, Polymer Symposium 63, 365.

Ziabicki, A., 1974. Generalized theory of nucleation kinetics III. Nucleation in dilute systems.. Colloid and Polymer Science 252, 207.